



# Structural, electronic and magnetic properties of electron-doped CrAs

B.S. Jacobs<sup>a,\*</sup>, Abhishek Pandey<sup>b,c</sup>

<sup>a</sup> Department of Physics, University of Johannesburg, Johannesburg 2006, Gauteng, South Africa

<sup>b</sup> Materials Physics Research Institute, School of Physics, University of the Witwatersrand, Johannesburg 2000, Gauteng, South Africa

<sup>c</sup> Ames Laboratory, Iowa State University, Ames 50011, IA, USA

## ARTICLE INFO

### Keywords:

Transition metal pnictides  
Chromium arsenide  
Electrical resistivity  
Magnetic susceptibility

## ABSTRACT

We report the effect of electron doping in binary transition metal-pnictide compound CrAs in polycrystalline compositions  $(\text{Cr}_{0.85}\text{T}_{0.15})\text{As}$  ( $T = \text{Fe}, \text{Co}, \text{Ni}$ ). Room temperature powder x-ray diffraction measurements show that the impurity-free doped samples crystallize in the orthorhombic MnP-type crystal structure with space group  $Pnma$ . Electrical resistivity  $\rho(T)$  data of all three compositions exhibit metallic behaviour with the room temperature  $\rho$  of about  $1 \text{ m}\Omega \text{ cm}$ , which is close to the values observed in single-crystal and polycrystalline samples of CrAs. Magnetic susceptibility  $\chi(T)$  data of all three compositions show paramagnetic behaviour and show no evidence any magnetic ordering down to 1.8 K. The  $\rho(T)$  and  $\chi(T)$  results collectively reveal that the antiferromagnetic ordering observed at Néel temperature  $T_N \approx 270 \text{ K}$  in CrAs is absent in the doped samples.

## 1. Introduction

Transition metal pnictides are an important family of compounds with several applications in photovoltaics [1], spin-dependent transport [2] and optoelectronics [3] to name a few. The discovery of superconductivity (SC) in iron-based layered compound  $\text{LaFeAsO}_{1-x}\text{F}_x$  with transition temperature ( $T_c$ ) of 26 K renewed interest in these materials [4]. Subsequently, several families of iron-based superconductors were discovered [5–7] with  $T_c$  as high as 55 K in  $\text{SmFeAsO}_{1-x}\text{F}_x$  [8]. Charge-carrier as well as co-doping studies played an important role in the development of this field as the parent compounds of iron-based superconductors are not superconducting. The common ingredient among the different families of iron-based superconductors is the stacked square lattice of Fe ions tetrahedrally coordinated by pnictogen ( $Pn$ ) ions, together constituting  $\text{FePn}$  layers. The dependence of  $T_c$  on the tetrahedral bond angle [9] as well as the height of the pnictogen from the iron plane [10] suggest the importance of the environment around iron on SC, which is altered by doping.

Binary CrAs is an interesting system as it exhibits an interplay between lattice and magnetic structures and SC, where a spin reorientation transition induced by pressure results into anti-parallel alignment of nearest neighbour spins in the vicinity of SC [11]. The compound exhibits highly tuneable magnetic moment and its propagation vector [11]. CrAs, which is structurally similar to binary FeAs, crystallizes in the MnP-type structure and undergoes a first order antiferromagnetic

(AFM) transition at  $T_N \approx 270 \text{ K}$  [12,13] (also see [supplementary material](#)). SC on the verge of AFM ordering was discovered in single crystals of CrAs by the application of pressure [14]. The first order AFM transition is completely suppressed at critical pressure of about 8 kbar and bulk SC with  $T_c$  close to 2 K emerges, making it the first superconductor among the Cr-based compounds. The phase diagram of CrAs [14] is similar to that of other unconventional SC systems [5,15] in that the onset of SC is in the vicinity of a quantum critical point (QCP) suggesting that the AFM fluctuations near the critical pressure support unconventional Cooper pairing.

While application of pressure allows a cleaner way of tuning of a system from a high temperature ordered state to a critical point, it is equally interesting to investigate the effects of doping as a tuning parameter. Further, controlling the electron count through doping has been successful in achieving SC in related iron-arsenides. Suzuki and Ido [16] investigated  $\text{Cr}_{1-x}\text{M}_x\text{As}$  ( $M = \text{Fe}, \text{Co}, \text{Ni}, \text{Ti}, x \leq 0.1$ ) compounds to understand the effect of doping of 3d metals on the crystallographic and magnetic properties of CrAs. Approximate values of  $T_N$  of the samples were determined by observing the temperature change of the lattice parameters. It was suggested that magnetic ordering disappears at dopant-dependent concentrations ranging between about 5 to 10 %. In the present work, we investigate the structural, electronic and magnetic properties of polycrystalline compositions  $(\text{Cr}_{0.85}\text{T}_{0.15})\text{As}$  ( $T = \text{Fe}, \text{Co}, \text{Ni}$ ) and attempt to compare the results with the parent CrAs. Our results suggest that doping suppresses the AFM ordering observed at 270 K in

\* Corresponding author.

E-mail addresses: [sjacobs@uj.ac.za](mailto:sjacobs@uj.ac.za) (B.S. Jacobs), [abhishek.pandey@wits.ac.za](mailto:abhishek.pandey@wits.ac.za) (A. Pandey).

<https://doi.org/10.1016/j.jmmm.2023.171397>

Received 23 July 2023; Received in revised form 2 October 2023; Accepted 16 October 2023

Available online 19 October 2023

0304-8853/© 2023 Elsevier B.V. All rights reserved.

CrAs as it evidently remains absent down to 1.8 K. We, however, do not find any evidence of SC in these doped compositions.

## 2. Experimental techniques

Polycrystalline  $(\text{Cr}_{0.85}\text{T}_{0.15})\text{As}$  ( $T = \text{Fe, Co, Ni}$ ) were synthesized by solid state reaction method using Cr (99.99 %), As (99.99999 %), Fe (99.998 %), Co (99.998 %) and Ni (99.9 %) from Alfa Aesar as the starting materials. Stoichiometric quantities of the starting materials were powdered and pressed into a pellet, placed in alumina crucible and sealed in a quartz tube under partial Ar pressure of about 0.25 atm. The sealed tubes were placed in a furnace and heated from room temperature to 585 °C in 10 h and held at this temperature for 20 h. It was then further heated to 620 °C in 5 h and kept at this temperature for 20 h, after which it was furnace cooled to room temperature. The samples were removed from tube, ground and pelletized again and annealed for a second time using the same temperature sequence as above up to 620 °C. It was then further heated to 1000 °C in 20 h and kept this temperature for 25 h, following which the tubes were removed from the furnace at 600 °C. Single crystal growth of undoped and doped CrAs were also attempted using the solution growth technique in Sn flux with the sample to Sn ratio of 1:25 using the same high quality starting materials. Stoichiometric quantities of the starting materials were placed in alumina crucibles and sealed in quartz tubes under slight Ar pressure of 0.25 atm. The tubes were placed in a furnace and heated to 1100 °C in 20 h, kept at this temperature for 50 h, slow cooled in 120 h to 700 °C and centrifuged. Needle-like single crystals of CrAs were obtained. However, the attempts to grow single crystals for the Fe, Co and Ni doped CrAs were unsuccessful. Room temperature powder x-ray diffraction (XRD) measurements on the doped polycrystalline samples were performed using a Rigaku Geigerflex powder diffractometer in Bragg Brentano geometry using  $\text{Cu-K}\alpha$  radiation. The diffractometer is equipped with a graphite monochromator and a scintillation type detector. Rietveld refinement was done using the FullProf package [17]. Four-probe temperature dependent electrical resistivity measurements were performed using a Physical Properties Measurement System of Quantum Design Inc. (QDI), USA. Temperature dependence of magnetic susceptibility as well as field dependence of isothermal magnetization were measured using a SQUID magnetometer of QDI.

## 3. Results and discussion

Fig. 1 shows the room temperature XRD pattern for  $(\text{Cr}_{0.85}\text{Fe}_{0.15})\text{As}$ ,  $(\text{Cr}_{0.85}\text{Co}_{0.15})\text{As}$  and  $(\text{Cr}_{0.85}\text{Ni}_{0.15})\text{As}$ . Our results show that all three compositions are in single phase with no detectable impurities. The compounds crystallise in the MnP-type orthorhombic structure with space group  $Pnma$  (SG No: 62). The refined unit cell parameters are listed in Table 1. It is important to mention that while the binary NiAs crystallizes in a hexagonal structure with space group  $P6_3/mmc$  (SG No: 194) which is different from the MnP-type orthorhombic structure

**Table 1**

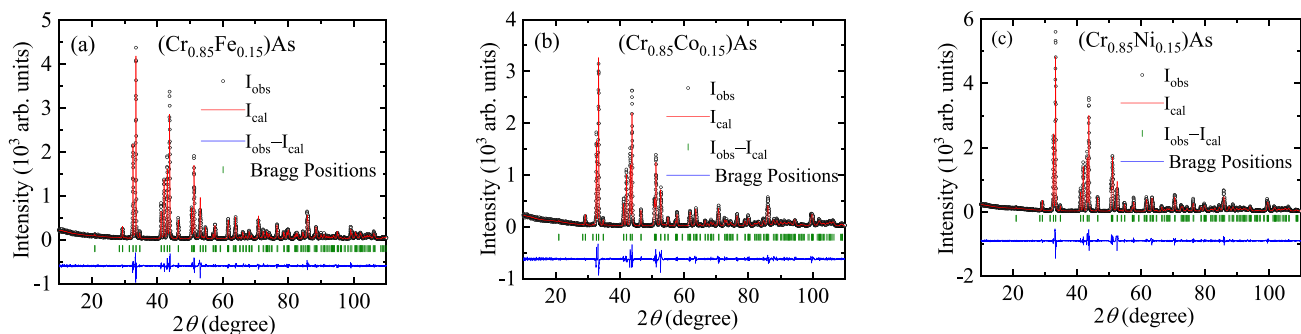
Structural parameters of polycrystalline  $(\text{Cr}_{0.85}\text{T}_{0.15})\text{As}$  ( $T = \text{Fe, Co, Ni}$ ). The listed crystallographic parameters are the unit cell parameters  $a$ ,  $b$  and  $c$  of the MnP-type orthorhombic structure ( $Pnma$ , No: 62) for the three compositions. The atomic positions of the transition metals  $T$  as well as that of As are also listed together with the reliability parameters  $R_F$ ,  $R_B$  and  $\chi^2$ .

Parameter	$(\text{Cr}_{0.85}\text{Fe}_{0.15})\text{As}$	$(\text{Cr}_{0.85}\text{Co}_{0.15})\text{As}$	$(\text{Cr}_{0.85}\text{Ni}_{0.15})\text{As}$
$a$ (Å)	5.6166(2)	5.5885(3)	5.5884(6)
$b$ (Å)	3.4218(1)	3.4466(2)	3.4546(1)
$c$ (Å)	6.1990(2)	6.1812(3)	6.1918(2)
$T_x$	0.0065(3)	0.0041(4)	0.0041(4)
$T_y$	0.25(0)	0.25(0)	0.25(0)
$T_z$	0.2011(3)	0.2017(3)	0.2016(3)
$\text{As}_x$	0.1999(3)	0.2012(3)	0.2012(2)
$\text{As}_y$	0.25(0)	0.25(0)	0.25(0)
$\text{As}_z$	0.5758(2)	0.5768(2)	0.5757(2)
$R_F$	3.74	3.72	4.42
$R_B$	6.09	6.28	7.08
$\chi^2$	2.56	2.84	3.56

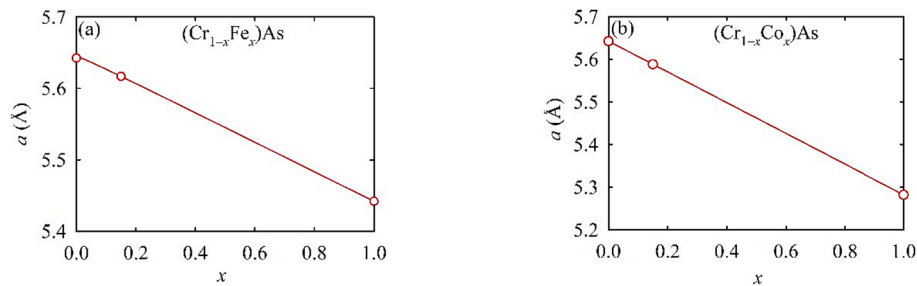
adopted by CrAs, FeAs and CoAs, it shows full solubility with CrAs as evident by the clean XRD pattern observed for  $(\text{Cr}_{0.85}\text{Ni}_{0.15})\text{As}$ .

Fig. 2 shows the variation of lattice parameter  $a$  with Fe and Co content  $x$  for the  $(\text{Cr}_{1-x}\text{Fe}_x)\text{As}$  and  $(\text{Cr}_{1-x}\text{Co}_x)\text{As}$  compositions. The linear dependence of  $a$  on  $x$  is in accordance with Vegard's law [18], which affirms the solubility as well as the good quality of the materials. Vegard's law could not be tested for the Ni-doped CrAs composition as the crystal structure of NiAs is different from the orthorhombic crystal structure of  $(\text{Cr}_{0.85}\text{Ni}_{0.15})\text{As}$ .

The temperature  $T$  dependence of electrical resistivity  $\rho$  for the  $(\text{Cr}_{0.85}\text{Fe}_{0.15})\text{As}$ ,  $(\text{Cr}_{0.85}\text{Co}_{0.15})\text{As}$  and  $(\text{Cr}_{0.85}\text{Ni}_{0.15})\text{As}$  compositions are shown in Fig. 3. The  $\rho(T)$  of three compounds show metallic behaviour with no evidence of any phase transition down to the lowest temperature of our measurements. Apparently, the transition observed at  $T_N \approx 270$  K in CrAs [12,13] is suppressed in these doped compounds. The room temperature  $\rho(T)$  of these compounds are  $\sim 1$  to 2 m $\Omega$  cm, which is similar to the values obtained for the single crystal as well polycrystalline samples of undoped CrAs (see the supplementary material) suggesting that these high-values are likely not related to the grain boundary effects. Despite exhibiting metallic behavior at high temperatures, the  $\rho(T)$  of all three compositions are very different from that of the parent binary compound CrAs. Unlike the quadratic temperature dependence observed at low temperature in CrAs suggesting for a Fermi liquid behavior below 15 K [19,20], the  $\rho(T)$  of  $(\text{Cr}_{0.85}\text{Fe}_{0.15})\text{As}$  and  $(\text{Cr}_{0.85}\text{Co}_{0.15})\text{As}$  show anomalous features where they exhibit shallow minima centred at 10 and 5 K, respectively, below which  $\rho$  increases with the decrease in  $T$  [Insets Fig. 3(a) and (b)]. Small span of temperature below the respective anomalies does not allow any meaningful analysis, but apparently this behavior could originate from Kondo-like effect due to the presence of small amounts of magnetic impurities in the lattice [21].



**Fig. 1.** Room temperature powder X-ray diffraction data of (a)  $(\text{Cr}_{0.85}\text{Fe}_{0.15})\text{As}$ , (b)  $(\text{Cr}_{0.85}\text{Co}_{0.15})\text{As}$  and (c)  $(\text{Cr}_{0.85}\text{Ni}_{0.15})\text{As}$  together with their Rietveld refinement and difference profiles as well as the Bragg positions.



**Fig. 2.** Variation of lattice parameter  $a$  with Fe and Co content  $x$  for (a)  $(\text{Cr}_{1-x}\text{Fe}_x)\text{As}$  and (b)  $(\text{Cr}_{1-x}\text{Co}_x)\text{As}$ . Solid lines are the guide to the eye. Error bars are smaller than the size of the symbols.

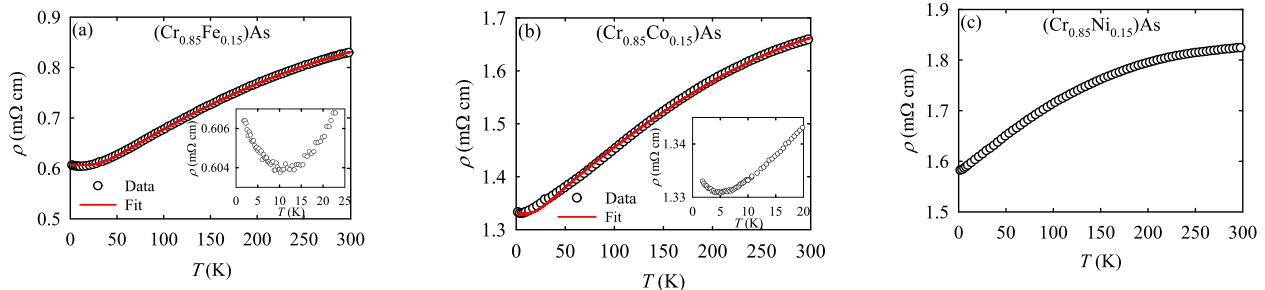


**Fig. 3.** Temperature  $T$  dependence of electrical resistivity  $\rho$  for (a)  $(\text{Cr}_{0.85}\text{Fe}_{0.15})\text{As}$ , (b)  $(\text{Cr}_{0.85}\text{Co}_{0.15})\text{As}$  and (c)  $(\text{Cr}_{0.85}\text{Ni}_{0.15})\text{As}$  compounds. Solid red curves in (a) and (b) are fits by equation (1). Insets in (a) and (b) show the minima observed in  $\rho$  at low temperatures.

The  $\rho(T)$  of  $(\text{Cr}_{0.85}\text{Fe}_{0.15})\text{As}$  and  $(\text{Cr}_{0.85}\text{Co}_{0.15})\text{As}$  could be fitted with the Bloch-Grüneisen-Mott model given by [19];

$$\rho(T) = \rho_0 + \rho_{\text{BG}}(T) - DT^3. \quad (1)$$

$\rho_{\text{BG}}(T)$  is the contribution predicted by Bloch-Grüneisen (BG) model of conduction carrier scattering by longitudinal lattice vibrations in the absence of umklapp processes [22]. According to the BG model, at high temperatures ( $T \geq \Theta_R$ ), where  $\Theta_R$  is Debye temperature,  $\rho_{\text{BG}}(T)$  is proportional to  $T$ . However, the data  $\rho(T)$  of the  $(\text{Cr}_{0.85}\text{Fe}_{0.15})\text{As}$  and  $(\text{Cr}_{0.85}\text{Co}_{0.15})\text{As}$  samples show negative curvature at high  $T$ . As a result, the Mott interband  $sd$ -scattering term proportion to  $T^3$  [23,24] was used in eq (1) to fit the data to account for this negative curvature. The fit parameters  $\Theta_R$  and  $D$  for the  $(\text{Cr}_{0.85}\text{Fe}_{0.15})\text{As}$  and  $(\text{Cr}_{0.85}\text{Co}_{0.15})\text{As}$  are listed in Table 2. This model, however, could not be used to fit the  $\rho(T)$  data of  $(\text{Cr}_{0.85}\text{Ni}_{0.15})\text{As}$  as they do not follow the expectations the BG model at low temperatures that leads to a  $T^5$  dependence. Instead, the  $\rho(T)$  data of this composition show a nearly linear behaviour below  $\sim 50$  K. This anomalous behaviour needs further investigations.

Fig. 4 shows the  $T$  dependence of magnetic susceptibility  $\chi$  for the  $(\text{Cr}_{0.85}\text{Fe}_{0.15})\text{As}$ ,  $(\text{Cr}_{0.85}\text{Co}_{0.15})\text{As}$  and  $(\text{Cr}_{0.85}\text{Ni}_{0.15})\text{As}$  compounds. No transition is observed down to the lowest temperature of measurement (see also derivative plots of magnetic susceptibility in supplementary material). The  $\chi(T)$  of the Fe-, Co- and Ni-doped samples exhibit a monotonic increase with the decrease of  $T$  with a tendency to saturation

**Table 2**

Physical properties parameters of polycrystalline  $(\text{Cr}_{0.85}\text{T}_{0.15})\text{As}$  ( $T = \text{Fe, Co, Ni}$ ). The listed physical properties parameters are Debye temperature  $\Theta_R$  deduced from resistivity  $\rho(T)$  data, coefficient  $D$  of  $T^3$  term in  $\rho(T)$ , Curie temperature  $\theta_p$ , Curie constant  $C$ , fit parameter  $\chi_0$  and calculated effective moment  $\mu_{\text{eff}}$ .

Parameter	$(\text{Cr}_{0.85}\text{Fe}_{0.15})\text{As}$	$(\text{Cr}_{0.85}\text{Co}_{0.15})\text{As}$	$(\text{Cr}_{0.85}\text{Ni}_{0.15})\text{As}$
$\Theta_R$ (K)	215.8(6)	127.6(1)	–
$D$ ( $\Omega \text{ cm}/\text{K}^3$ )	$1.84(1) \times 10^{-12}$	$3.23(4) \times 10^{-12}$	–
$\theta_p$ (K)	60(15)	–28(11)	66(24)
$C$ ( $\text{cm}^3 \text{ K}/\text{mol}$ )	0.5(1)	0.15(2)	0.011(4)
$\chi_0$ ( $\text{cm}^3/\text{mol}$ )	0	$8.1(3) \times 10^{-4}$	$9.1(2) \times 10^{-4}$
$\mu_{\text{eff}}$ ( $\mu_B$ )	2.0(2)	1.09(7)	0.29(5)

observed in Fe- and Co- doped compounds below about 15 K. These features are entirely different from the  $\chi(T)$  of undoped CrAs where latter undergoes an AFM ordering at  $\sim 270$  K and then exhibits a monotonic decrease with the further decrease of temperature (see supplementary material). Additionally, the high-temperature  $\chi(T)$  data of the Fe- Co- and Ni-doped compositions show Curie-Weiss (CW) like behaviour above 100, 50 and 150 K, respectively, and were fitted using the modified CW equation;

$$\chi = \frac{C}{T - \theta_p} + \chi_0, \quad (2)$$

where  $C$  is the Curie constant,  $\theta_p$  is the Curie temperature and  $\chi_0$  is a temperature-independent term which accounts for the contribution from the inherent defects in the samples. Apparently below the temperatures mentioned above, short range magnetic correlations start to develop and as a result, the susceptibility deviates from modified CW behaviour. The fit parameters are listed in Table 2 together with the calculated values of the effective paramagnetic moment  $\mu_{\text{eff}}$ .

The positive  $\theta_p$  obtained for Fe- and Ni-doped compositions indicates the dominance of ferromagnetic (FM) interactions in these materials whereas the estimated negative value for the Co-doped sample infers the predominance of the AFM interactions. The partial substitution of Cr by Fe and Ni is equivalent to introducing an even number of extra electrons, two and four respectively, in presumably highly hybridized transition metal pnicride bands. On the other hand, substitution by Co contributes three extra electrons. Apparently, the change in carrier density significantly alters the balance of the underlying competing magnetic interactions leading to a crossover of the dominance of FM interaction to AFM with the variation of the dopant.

Fig. 5 shows isothermal magnetization  $M$  as a function of applied magnetic field  $H$  measured at seven different temperatures between 1.8 and 300 K for  $(\text{Cr}_{0.85}\text{Fe}_{0.15})\text{As}$ ,  $(\text{Cr}_{0.85}\text{Co}_{0.15})\text{As}$  and  $(\text{Cr}_{0.85}\text{Ni}_{0.15})\text{As}$ . The  $M(H)$  data show a nearly linear variation of  $M$  with  $H$  at high temperatures ( $T \geq 100$  K), but the data measured at low temperatures, roughly below 50 K, exhibit a curvature. This behaviour is expected from the paramagnetic spins when the magnetic energy  $\mu H$  becomes comparable to thermal fluctuations  $k_B T$  as described by Brillouin function (BF) [25].

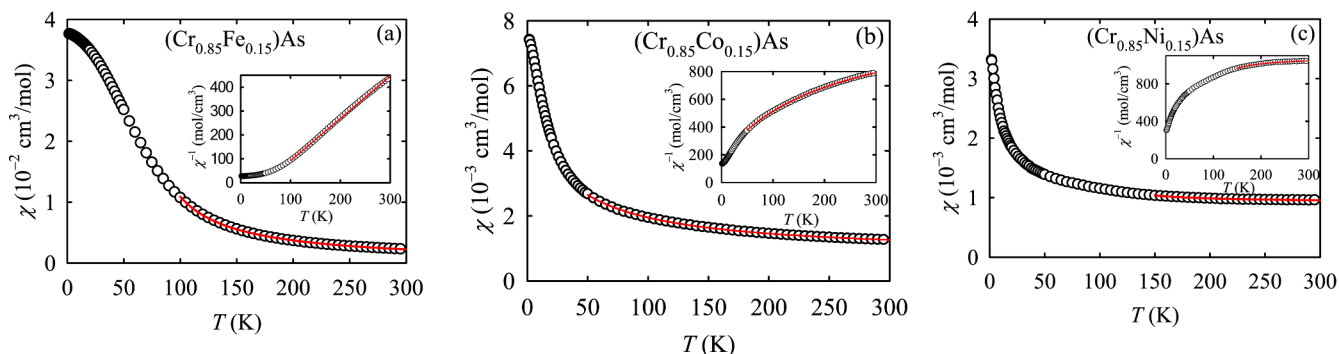


**Fig. 4.** Temperature dependence of magnetic susceptibility  $\chi$  for (a)  $(\text{Cr}_{0.85}\text{Fe}_{0.15})\text{As}$ , (b)  $(\text{Cr}_{0.85}\text{Co}_{0.15})\text{As}$  and (c)  $(\text{Cr}_{0.85}\text{Ni}_{0.15})\text{As}$  compounds. Insets in (a), (b) and (c) show the temperature dependence of inverse magnetic susceptibility. Solid red curves are fits by equation (2).

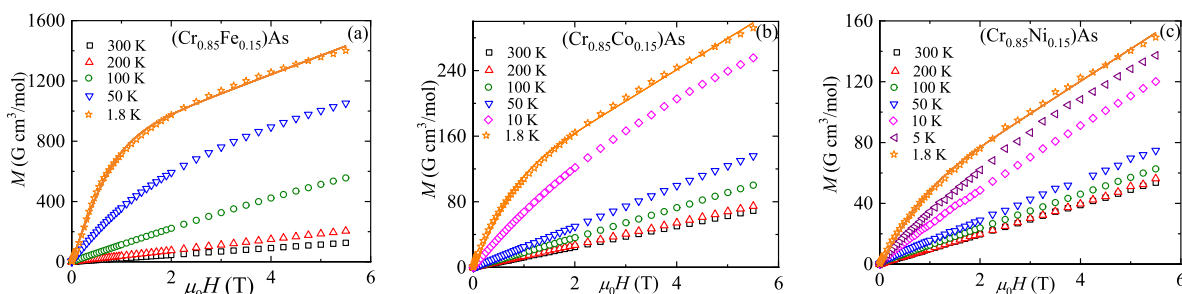


**Fig. 5.** Field dependence of isothermal magnetization  $M$  versus applied magnetic field  $H$  for  $(\text{Cr}_{0.85}\text{Fe}_{0.15})\text{As}$ ,  $(\text{Cr}_{0.85}\text{Co}_{0.15})\text{As}$  and  $(\text{Cr}_{0.85}\text{Ni}_{0.15})\text{As}$  compounds at seven different temperatures. The  $M(H)$  data of the Fe-doped material at 5 and 10 K are not shown in (a) as they overlap with the 1.8 K data. Similarly, the  $M(H)$  data of the Co-doped material at 5 K are not shown in (b). The solid curves are fits to  $T = 1.8$  K data by equation (3) as discussed in the text.

To explore it further, we fitted the  $M(H)$  data at  $T = 1.8$  K of all the three compositions using the expression,

$$M(T, H) = fM_{\text{sat}}B_S \left[ \frac{g\mu_B H}{k_B T} \right] + \chi_L H, \quad (3)$$

where  $B_S$  is BF,  $M_{\text{sat}} = N_{\text{Ag}}S\mu_B$ ,  $f$  is the prefactor to the BF defining the concentration of the paramagnetic ions and  $\chi_L$  is the linear susceptibility. To avoid over parametrization, we kept the value of  $f$  fixed at 0.15 and only varied two parameters  $\chi_L$  and  $S$  and got reasonably good fits to the data [Fig. 5]. The fitted values of the parameters  $\chi_L$  in  $\text{G cm}^3/\text{mol}$  &  $S$ , in that order, are the following for Fe-, Co- and Ni-doped samples: 0.0126(3) & 0.441(6); 0.0041(6) & 0.056(2); 0.00213(3) & 0.0210(6).

#### 4. Conclusion

A pure phase of polycrystalline materials  $(\text{Cr}_{0.85}\text{Fe}_{0.15})\text{As}$ ,  $(\text{Cr}_{0.85}\text{Co}_{0.15})\text{As}$  and  $(\text{Cr}_{0.85}\text{Ni}_{0.15})\text{As}$  were successfully synthesized without any detectable impurities. Temperature dependence of electrical resistivity and magnetic susceptibility show no evidence of magnetic ordering down to the lowest temperature 1.8 K of our measurements despite the sizeable values of magnetic interactions present in the compounds. Apparently, the antiferromagnetic transition observed at  $T_N \approx 270$  K in undoped CrAs gets suppressed by low-doping concentrations of Fe, Co and Ni. Interestingly, while we observe the presence of predominant ferromagnetic interactions in the Fe- and Ni-doped materials, the dominant interactions in the Co-doped material are apparently antiferromagnetic in nature. The low-temperature resistivities of the doped compositions are markedly different from the parent correlated metal CrAs which exhibits Fermi liquid behavior. Additionally, the resistivities of Fe- and Co-doped compound exhibit minima below sample-dependent temperatures. The observed, minima in these compounds correlate with the onset of saturation observed in

the magnetic susceptibilities, suggesting for a common origin of the two phenomena. No superconductivity was observed. As superconductivity emerges in the vicinity of antiferromagnetic interactions, samples with lower dopant amounts may be investigated in the future. Additionally, it would also be interesting to investigate the effect of hole doping introduced by partial substitution of Cr by Sc, Ti and V.

#### Declaration of Competing Interest

The authors declare that they have no known competing financial interests or personal relationships that could have appeared to influence the work reported in this paper.

#### Data availability

Data will be made available on request.

#### Acknowledgements

This work is based on the research supported in part by the National Research Foundation of South Africa (Ref Numbers: SRUG2205098188 and 138329). A.P. acknowledges the financial support from the Friedel Sellschop fellowship of the University of the Witwatersrand, South Africa. The work at Ames Laboratory was supported by the U.S. Department of Energy, Office of Basic Energy Sciences, Division of Materials Sciences and Engineering. Ames Laboratory is operated for the U.S. Department of Energy by Iowa State University under Contract No. DE-AC02-07CH11358.

#### Appendix A. Supplementary data

Supplementary data to this article can be found online at <https://doi.org/10.1016/j.jmmm.2023.171397>.

## References

- [1] C. Tablero, A.J. García, J.J. Fernández, P. Palacios, P. Wahnón, *Comput. Mater. Sci.* 27 (2003) 58.
- [2] M.S. Brandt, S.T.B. Goennenwein, T. Graf, H. Huebl, S. Lauterbach, M. Stutzmann, *Phys. Status Solidi C* 1 (2004) 2056.
- [3] S.E. Mohny, *J. Electron. Mater.* 27 (1998) 26.
- [4] Y. Kamihara, T. Watanabe, M. Hirano, H. Hosono, *J. Am. Chem. Soc.* 130 (2008) 3296.
- [5] J. Paglione, R.L. Greene, *Nature Phys.* 6 (2010) 645.
- [6] D.C. Johnston, *Adv. Phys.* 59 (2010) 803.
- [7] G.R. Stewart, *Rev. Mod. Phys.* 83 (2011) 1589.
- [8] Z.-A. Ren, W. Lu, J. Yang, W. Yi, X.-L. Shen, Z. Li, G.-C. Che, X.-L. Dong, L.-L. Sun, F. Zhou, Z. Zhao, *Chin. Phys. Lett.* 25 (2008) 2215.
- [9] C.H. Lee, A. Iyo, H. Eisaki, H. Kito, M. Fernandez-Diaz, T. Ito, K. Kihou, H. Matsuhata, M. Braden, K. Yamada, *J. Phys. Soc. Jpn.* 77 (2008), 083704.
- [10] K. Kuroki, H. Usui, S. Onari, R. Arita, H. Aoki, *Phys. Rev. B* 79 (2009), 224511.
- [11] Y. Shen, Q. Wang, Y. Hao, B. Pan, Y. Feng, Q. Huang, L.W. Harriger, J.B. Leao, Y. Zhao, R.M. Chisnell, J.W. Lynn, H. Cao, J. Hu, J. Zhao, *Phys. Rev. B* 93 (2016) 06503(R).
- [12] H. Watanabe, N. Kazama, Y. Yamaguchi, M. Ohashi, *J. Appl. Phys.* 40 (1969) 1128.
- [13] K. Selte, A. Kjekshus, W.E. Jamison, A.F. Andresen, J.E. Engebretsen, *Acta Chem. Scand.* 25 (1971) 1703.
- [14] W. Wu, J. Cheng, K. Matsubayashi, P. Kong, F. Lin, C. Jin, N. Wang, Y. Uwatoko, J. Luo, *Nat. Commun.* 5 (2014) 5508.
- [15] K. Jin, N.P. Butch, K. Kirshenbaum, K. Paglione, R.L. Greene, *Nature* 476 (2011) 73.
- [16] T. Suzuki, H. Ido, *J. Appl. Phys.* 69 (1991) 4624.
- [17] J. Rodríguez-Carvajal, *Phys. B Condens. Matter* 192 (1993) 55.
- [18] A.R. Denton, N.W. Ashcroft, *Phys. Rev. A* 43 (1991) 3161.
- [19] J. Cheng, J. Luo, *J. Phys. Condens. Matter* 29 (2017), 383003.
- [20] W. Wu, X.D. Zhang, Z.H. Yin, P. Zheng, N.L. Wang, J.L. Luo, *Sci. China Phys. Mech. Astron.* 53 (2010) 1207.
- [21] A. Pandey, C. Mazumdar, R. Ranganathan, *J. Alloy. Compd.* 476 (2009) 14.
- [22] A. Pandey, D.G. Quirinale, W. Jayasekara, A. Sapkota, M.G. Kim, R.S. Dhaka, Y. Lee, T.W. Heitmann, P.W. Stephens, V. Oglobichev, A. Kreyssig, R. J. McQueeney, A.I. Goldman, A. Kaminski, B.N. Harmon, Y. Furukawa, D. C. Johnston, *Phys. Rev. B* 88 (2013), 014526.
- [23] N.F. Mott, *Proc. Roy. Soc. London A* 153 (1936) 699.
- [24] M. Giovannini, H. Michor, E. Bauer, G. Hilscher, P. Rogl, *J. Alloy. Compd.* 280 (1998) 26.
- [25] A. Pandey, P. Miao, M. Klemm, H. He, H. Wang, X. Qian, J.W. Lynn, M.C. Aronson, *Phys. Rev. B* 102 (2020), 014406.